

# Wavelength calibration of a high resolution spectrograph with a partially stabilized 15-GHz astrocomb from 550 to 890 nm

RICHARD A. MCCrackEN,<sup>1,\*</sup> ÉRIC DEPAGNE,<sup>2</sup> RUDOLF B. KUHN,<sup>2</sup> NICOLAS ERASMUS,<sup>2</sup> LISA A. CRAUSE,<sup>2</sup> AND DERRYCK T. REID<sup>1</sup>

<sup>1</sup>Scottish Universities Physics Alliance (SUPA), Institute of Photonics and Quantum Sciences, School of Engineering and Physical Sciences, Heriot-Watt University, Edinburgh EH14 4AS, UK

<sup>2</sup>South African Astronomical Observatory, P.O. Box 9, Observatory 7935, Cape Town, South Africa

\*R.A.McCracken@hw.ac.uk

**Abstract:** A visible astrocomb spanning 555–890 nm has been implemented on the 10-m Southern African Large Telescope, delivering complete calibration of one channel of its high-resolution spectrograph and an accurate determination of its resolving power. A novel co-coupling method allowed simultaneous observation of on-sky, Th-Ar lamp and astrocomb channels, reducing the wavelength calibration uncertainty by a factor of two compared to that obtained using only Th-Ar lines. The excellent passive stability of the master frequency comb laser enabled broadband astrocomb generation without the need for carrier-envelope offset frequency locking, and an atomically referenced narrow linewidth diode laser provided an absolute fiducial marker for wavelength calibration. The simple astrocomb architecture enabled routine operation by non-specialists in an actual telescope environment. On-sky spectroscopy results are presented with direct calibration achieved entirely using the astrocomb.

Published by The Optical Society under the terms of the [Creative Commons Attribution 4.0 License](https://creativecommons.org/licenses/by/4.0/). Further distribution of this work must maintain attribution to the author(s) and the published article's title, journal citation, and DOI.

**OCIS codes:** (120.6200) Spectrometers and spectroscopic instrumentation; (350.1260) Astronomical optics.

## References and links

1. D. A. Fischer, G. Anglada-Escude, P. Arriagada, R. V. Baluev, J. L. Bean, F. Bouchy, L. A. Buchhave, T. Carroll, A. Chakraborty, J. R. Crepp, R. I. Dawson, S. A. Diddams, X. Dumusque, J. D. Eastman, M. Endl, P. Figuera, E. B. Ford, D. Foreman-Mackey, P. Fournier, G. Furesz, B. Scott Gaudi, P. C. Gregory, F. Grundahl, A. P. Hatzes, G. Hebrard, E. Herrero, D. W. Hogg, A. W. Howard, J. A. Johnson, P. Jorden, C. A. Jurgenson, D. W. Latham, G. Laughlin, T. J. Loredo, C. Lovis, S. Mahadevan, T. M. McCracken, F. Pepe, M. Perez, D. F. Phillips, P. P. Plavchan, L. Prato, A. Quirrenbach, A. Reiners, P. Robertson, N. C. Santos, D. Sawyer, D. Segransan, A. Sozzetti, T. Steinmetz, A. Szentgyorgyi, S. Udry, J. A. Valenti, S. X. Wang, R. A. Wittenmyer, and J. T. Wright, "State of the field: extreme precision radial velocities," *Publ. Astron. Soc. Pac.* **128**(964), 066001 (2016).
2. F. Quinlan, G. Ycas, S. Osterman, and S. A. Diddams, "A 12.5 GHz-spaced optical frequency comb spanning >400 nm for near-infrared astronomical spectrograph calibration," *Rev. Sci. Instrum.* **81**(6), 063105 (2010).
3. G. G. Ycas, F. Quinlan, S. A. Diddams, S. Osterman, S. Mahadevan, S. Redman, R. Terrien, L. Ramsey, C. F. Bender, B. Botzer, and S. Sigurdsson, "Demonstration of on-sky calibration of astronomical spectra using a 25 GHz near-IR laser frequency comb," *Opt. Express* **20**(6), 6631–6643 (2012).
4. T. Wilken, C. Lovis, A. Manescau, T. Steinmetz, L. Pasquini, G. Lo Curto, T. W. Hansch, R. Holzwarth, and T. Udem, "High-precision calibration of spectrographs," *Mon. Not. R. Astron. Soc. Lett.* **405**(1), 16–20 (2010).
5. T. Wilken, G. L. Curto, R. A. Probst, T. Steinmetz, A. Manescau, L. Pasquini, J. I. González Hernández, R. Rebolo, T. W. Hänsch, T. Udem, and R. Holzwarth, "A spectrograph for exoplanet observations calibrated at the centimetre-per-second level," *Nature* **485**(7400), 611–614 (2012).
6. D. A. Braje, M. S. Kirchner, S. Osterman, T. Fortier, and S. A. Diddams, "Astronomical spectrograph calibration with broad-spectrum frequency combs," *Eur. Phys. J. D* **48**(1), 57–66 (2008).
7. C.-H. Li, A. J. Benedick, P. Fendel, A. G. Glenday, F. X. Kärtner, D. F. Phillips, D. Sasselov, A. Szentgyorgyi, and R. L. Walsworth, "A laser frequency comb that enables radial velocity measurements with a precision of 1 cm s<sup>-1</sup>," *Nature* **452**(7187), 610–612 (2008).
8. C.-H. Li, A. G. Glenday, A. J. Benedick, G. Chang, L.-J. Chen, C. Cramer, P. Fendel, G. Furesz, F. X. Kärtner, S. Korzennik, D. F. Phillips, D. Sasselov, A. Szentgyorgyi, and R. L. Walsworth, "In-situ determination of astro-

- comb calibrator lines to better than 10 cm s<sup>-1</sup>,” *Opt. Express* **18**(12), 13239–13249 (2010).
9. A. G. Glenday, C.-H. Li, N. Langellier, G. Chang, L.-J. Chen, G. Furesz, A. A. Zibrov, F. Kärtner, D. F. Phillips, D. Sasselov, A. Szentgyorgyi, and R. L. Walsworth, “Operation of a broadband visible-wavelength astro-comb with a high-resolution astrophysical spectrograph,” *Optica* **2**(3), 250–254 (2015).
  10. A. J. Benedick, G. Chang, J. R. Birge, L. J. Chen, A. G. Glenday, C.-H. Li, D. F. Phillips, A. Szentgyorgyi, S. Korzennik, G. Furesz, R. L. Walsworth, and F. X. Kärtner, “Visible wavelength astro-comb,” *Opt. Express* **18**(18), 19175–19184 (2010).
  11. D. F. Phillips, A. G. Glenday, C.-H. Li, C. Cramer, G. Furesz, G. Chang, A. J. Benedick, L.-J. Chen, F. X. Kärtner, S. Korzennik, D. Sasselov, A. Szentgyorgyi, and R. L. Walsworth, “Calibration of an astrophysical spectrograph below 1 m/s using a laser frequency comb,” *Opt. Express* **20**(13), 13711–13726 (2012).
  12. C.-H. Li, G. Chang, A. G. Glenday, N. Langellier, A. Zibrov, D. F. Phillips, F. X. Kärtner, A. Szentgyorgyi, and R. L. Walsworth, “Conjugate Fabry-Perot cavity pair for improved astro-comb accuracy,” *Opt. Lett.* **37**(15), 3090–3092 (2012).
  13. T. Steinmetz, T. Wilken, C. Araujo-Hauck, R. Holzwarth, T. W. Hänsch, and T. Udem, “Fabry – Pérot filter cavities for wide-spaced frequency combs with large spectral bandwidth,” *Appl. Phys. B Lasers Opt.* **96**(2-3), 251–256 (2009).
  14. L. A. Crause, R. M. Sharples, D. G. Bramall, J. Schmoll, P. Clark, E. J. Younger, L. M. G. Tyas, S. G. Ryan, J. D. Brink, O. J. Strydom, D. A. H. Buckley, M. Wilkinson, S. M. Crawford, and E. Depagne, “Performance of the Southern African Large Telescope (SALT) High Resolution Spectrograph (HRS),” *Proc. SPIE* **9147**, 91476T (2014).
  15. Z. Zhang, K. Balskus, R. A. McCracken, and D. T. Reid, “Mode-resolved 10-GHz frequency comb from a femtosecond optical parametric oscillator,” *Opt. Lett.* **40**(12), 2692–2695 (2015).
  16. J. Ye, S. Swartz, P. Jungner, and J. L. Hall, “Hyperfine structure and absolute frequency of the (87)Rb 5P(3/2) state,” *Opt. Lett.* **21**(16), 1280–1282 (1996).
  17. R. A. McCracken, K. Balskus, Z. Zhang, and D. T. Reid, “Atomically referenced 1-GHz optical parametric oscillator frequency comb,” *Opt. Express* **23**(12), 16466–16472 (2015).
  18. M. T. Murphy, T. Udem, R. Holzwarth, A. Sizmman, L. Pasquini, C. Araujo-Hauck, H. Dekker, S. D’Odorico, M. Fischer, T. W. Hänsch, and A. Manescau, “High-precision wavelength calibration of astronomical spectrographs with laser frequency combs,” *Mon. Not. R. Astron. Soc.* **380**(2), 839–847 (2007).
  19. B. A. Palmer and R. Engleman, “Atlas of the Thorium spectrum,” Los Alamos Natl. Lab. Report, LA-9615 (1983).
  20. C. C. Thöne, J. Greiner, S. Savaglio, and E. Jehin, “ISM Studies of GRB 030329 with high-resolution spectroscopy,” *Astrophys. J.* **671**(1), 628–636 (2007).
  21. M. Endo, I. Ito, and Y. Kobayashi, “Direct 15-GHz mode-spacing optical frequency comb with a Kerr-lens mode-locked Yb:Y<sub>2</sub>O<sub>3</sub> ceramic laser,” *Opt. Express* **23**(2), 1276–1282 (2015).
  22. A. Bartels, D. Heinecke, and S. A. Diddams, “Passively mode-locked 10 GHz femtosecond Ti:sapphire laser,” *Opt. Lett.* **33**(16), 1905–1907 (2008).

## 1. Introduction

Astronomical spectrographs combining high resolution ( $R \gg 10,000$ ) with high stability provide unique scientific capabilities, e.g. for observing the small Doppler shifts which are signatures of Earth-like exoplanets or sensitively measuring isotopic ratios in ancient stars to reveal details of the early universe. For large telescopes, the accuracy of the calibration source rather than intrinsic photon noise limits the measurement precision. Conventionally, thorium-argon (Th-Ar) lamps are used to provide calibration lines in the visible region, but their non-uniform spectral coverage, wide intensity variations and lack of absolute traceability limit their suitability for the most demanding observations [1].

Multiple approaches have been taken in developing astrocombs in recent years. Er-fiber frequency combs operating at 250 MHz have been amplified, filtered and spectrally broadened to provide spectral coverage from 1400 to 1800 nm with mode spacings ranging from 12.5 to 25 GHz [2,3]. Using Yb: fiber this approach has been combined with an additional frequency doubling stage to generate an astrocomb spanning 450–600 nm [4,5]. These astrocombs harness the excellent comb stability of fiber lasers, however the lower native repetition frequency requires additional filtering to achieve the necessary mode spacing for spectrograph calibration. Achieving sufficient side-mode suppression therefore requires multiple amplification and filtering stages, which add complexity and increase the risk of damaging sensitive fiber components. Solid-state lasers can deliver femtosecond pulses at GHz repetition rates, reducing the demands on mode filtering and providing broadband outputs either directly or through spectral broadening in suitable nonlinear fiber. Some

astrocombs have used octave-spanning Ti:sapphire lasers, where the wide spectral coverage enables comb offset frequency locking without the need for photonic crystal fiber. Mode spacings from 30 to 50 GHz have been demonstrated in the near-infrared (780–1000 nm [6–8]), green (500–620 nm [9]) and blue (400–430 nm [10,11]) spectral regions. In each embodiment the astrocomb bandwidth has been limited by the performance of the mirror coatings in the Fabry-Pérot etalon used to filter the comb modes rather than the stability of the frequency comb. The filtering requirements are technically challenging: sideband suppression, asymmetry, and spectral flatness all impact the astrocomb performance when deployed on a spectrograph [12,13]. For this reason, on-sky calibration of a spectrograph using an astrocomb has been limited to modest instantaneous bandwidths, where the Fabry-Pérot etalon performance can be well defined.

Here we demonstrate practical calibration of on-sky spectrograph data from the 10-m Southern African Large Telescope (SALT) using a 15- to 25-GHz comb with instantaneous visible coverage from 550 to 900 nm. This broad spectral bandwidth makes it possible to completely calibrate the diffraction orders of the red channel (555–890 nm) of SALT's high-resolution échelle spectrograph (HRS). Since first-light commissioning of HRS in 2013, the instrument has lacked an accurate wavelength map of the cross-dispersed light in the near-infrared due to the scarcity of emission lines in this region from the Th-Ar calibration lamp [14]. The use of an astrocomb for the first time allows wavelength tagging of each CCD pixel, and by doing so can reveal systematic errors in the spectrograph calibration and accurately determine its actual resolution, including its wavelength dependence.

The reduced operational demands of this astrocomb, compared with those designed exclusively for precision radial velocity measurements, allow for simpler Fabry-Pérot etalon coatings and a partially stabilized master frequency comb. This has reduced the overall complexity of the astrocomb and enabled the system to be operated fully by astronomers with no prior laser experience.

## 2. System description

### 2.1 Laser frequency comb

The comb (Fig. 1, top panel) was based on a 1-GHz Ti:sapphire laser (Gigajet, Laser Quantum) producing 20-fs pulses centered at 807 nm and 1.2 W of average power. Approximately 60% of this output was launched into a 30-cm length of photonic crystal fiber (PCF, NL-750-PM, NKT Photonics) with 30% coupling efficiency, yielding supercontinuum generation from 550 to 900 nm (Fig. 2). The 1-GHz supercontinuum comb was filtered by a single pass of a Fabry-Pérot etalon, whose cavity comprised a complementary pair of dispersion minimizing mirrors (Laseroptik). A portion of the Ti:sapphire beam was sampled before entering the PCF and co-coupled into the Fabry-Pérot etalon with the supercontinuum with a small vertical offset. The etalon was dither-locked directly to the unbroadened Ti:sapphire comb [15], and was typically configured to provide a 15-GHz mode-spacing. Dither locking to the comb provided a tight lock with a RMS uncertainty in the mode spacing of 600 kHz, which is well below the 190-MHz linewidth of the etalon transmission function (see §2.3). The filtered comb was launched into a 10-m length of broadband single-mode PCF (aeroGUIDE-10-PM, NKT Photonics) for delivery to the calibration channel of HRS.

Fabry-Pérot filtering of a frequency comb produces an ambiguity in the exact frequencies of the filtered comb modes because it is possible to filter a different sub-set of modes from lock to lock. Several methods for providing absolute wavelength information have been demonstrated, including the use of a wavemeter [4], and a CW laser stabilized directly to a comb line for both Fabry-Pérot locking and as a mode guide [11]. Here, a narrow-linewidth single frequency diode laser (D2-100-DBR, Vescent Photonics) was dither-locked to the  $^{87}\text{Rb}$   $F = 2 \rightarrow F' = 2,3$  crossover (384,227,981.9 MHz [16]) and co-coupled into the PCF providing the supercontinuum. A small portion of the Rb-stabilized laser leaked through the stabilized

Fabry-Pérot etalon and launched into the spectrograph, providing an absolute fiducial marker for calibration.

The astrocomb was located within the spectrograph electronics control room at SALT, which houses multiple server stacks and is temperature controlled to within  $\pm 1.5^\circ\text{C}$ . No optical table was available on site, and so the astrocomb was constructed on a  $900 \times 900\text{-mm}$  lightweight aluminum breadboard supported by four compact air mounts for vibration isolation. A Perspex box provided isolation against currents from the air conditioning system in the room. As shown in the lower left panel of Fig. 1, the astrocomb was attached to a solid wooden base and placed on an office desk. Despite the lack of a controlled operating environment, the astrocomb was sufficiently stable for continuous overnight operation.

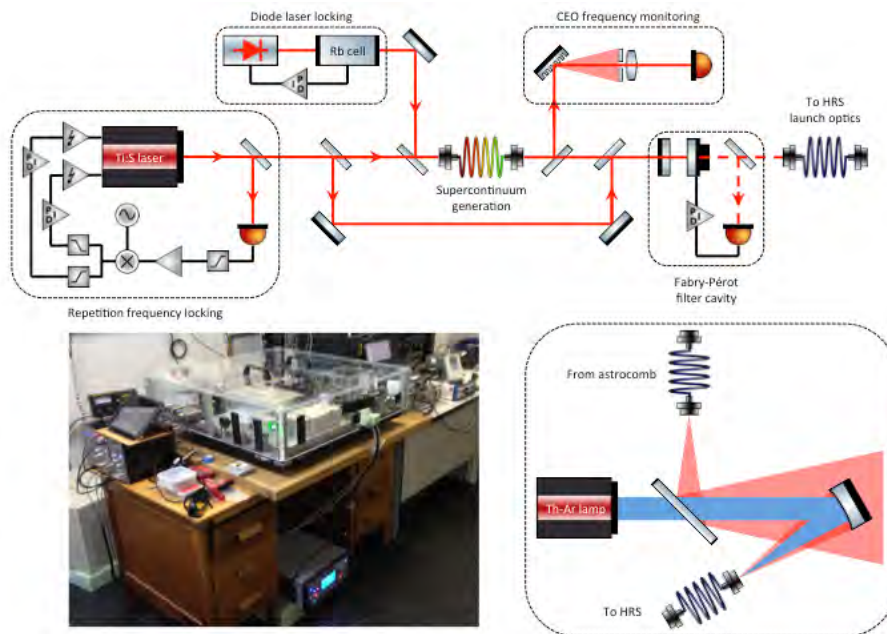


Fig. 1. Top, schematic of the astrocomb deployed at SALT; Left, the astrocomb in the electronic control room for HRS; Right, the dual-calibrator configuration for HRS.

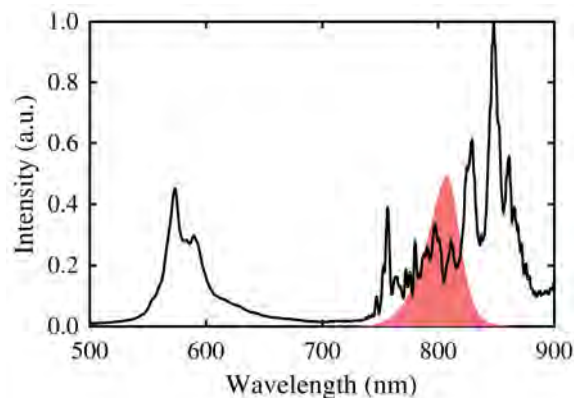


Fig. 2. Comb spectrum after the Fabry-Pérot etalon, with the spectrum of the Ti:sapphire comb used for cavity locking shown in red.

The configuration for coupling the astrocomb into HRS is shown in the lower right panel of Fig. 1. Comb light exiting the single-mode launch fiber was reflected off a  $45^\circ$  uncoated

quartz beam-splitter placed in front of the Th-Ar calibration lamp and subsequently coupled into the HRS input fiber. This enabled the simultaneous coupling of both calibration sources into one channel of the spectrograph, a capability which has not previously been reported, and which allows for accurate determination of the Th-Ar emission lines against the astrocomb reference. To prevent saturation of the spectrograph CCD by the comparatively intense astrocomb, the output from the single-mode launch fiber was not collimated. The small fraction of the rapidly diverging beam that was reflected by the beam-splitter into the HRS input fiber was sufficiently intense for comb lines to be observable over both short- and long-term exposures.

## 2.2 Frequency comb stability

A fraction of the Ti:sapphire laser beam was sampled with a beamsplitter and steered to a high-bandwidth GaAs photodiode (ET-4000, Electro-Optics Technology) in order to measure the repetition frequency ( $f_{\text{REP}}$ ). The 8th harmonic of this signal was filtered, amplified and mixed with a local reference oscillator (QuickSyn Lite FSL-0010, National Instruments), itself stabilized to a 10-MHz microwave clock (LCR-900, Spectratime). The output from the mixer was used as an error signal to stabilize  $f_{\text{REP}}$  through a pair of intracavity piezoelectric transducers (PZTs). The in-loop RMS error of the lock was 0.64 mHz over 1 s, corresponding to a contribution to the comb linewidth of 240 Hz from the reference electronics (Fig. 3(a)).

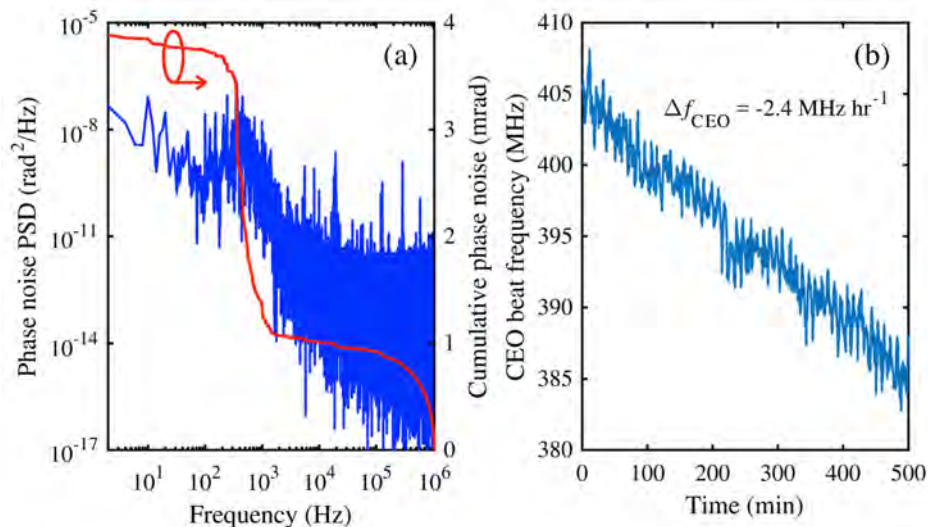


Fig. 3. (a) In-loop phase noise power spectral density measurement of the locked repetition frequency. The cumulative phase noise is 3.88 mrad over a 1-second observation window. (b) Measured drift in the Ti:sapphire carrier-envelope offset frequency over an 8-hour period.

Detection of the Ti:sapphire laser CEO frequency ( $f_{\text{CEO}}$ ) was carried out by heterodyning against the atomically-referenced diode laser [17]. Ideal spatial mode-matching was achieved by co-coupling the diode laser into the PCF used for supercontinuum generation. The fiber output was sampled before entering the Fabry-Pérot etalon and steered into a monochromator, with the  $f_{\text{CEO}}$  detected on a high-speed avalanche photodiode (APD210, Menlo Systems).

The stability of the Ti:sapphire frequency comb was determined by recording  $f_{\text{CEO}}$  at 30-second intervals over an 8-hour window while  $f_{\text{REP}}$  was locked. As shown in Fig. 3(b), the CEO frequency drifted by just 2% over the course of a night, with the drift arising primarily due to minute changes in the coupling of the CW pump to the Ti:sapphire laser, and room temperature cycling causing the smaller fluctuations. The corresponding 20-MHz shift in the position of a filtered comb line on the CCD array is only 0.3% of the spectrograph resolution

so is negligible, therefore active stabilization of  $f_{\text{CEO}}$  is not required, and was instead only monitored during nightly operation.

### 2.3 Fabry-Pérot etalon performance

The resolving power ( $\lambda/\Delta\lambda$ ) of HRS was previously measured to be  $R \approx 65,000$ , corresponding to an optical resolution of 5.8 GHz at 800 nm [14]. For optimal calibration a comb line should occur every  $\sim 2.5$  resolution elements on the spectrograph CCD [18], providing a high line density with minimal overlap between neighboring lines. The optimal spacing for HRS is therefore 15 GHz, easily achievable when starting with a 1-GHz pump laser.

The Fabry-Pérot etalon comprised a pair of mirrors with complementary coatings such that the net group delay across the operational bandwidth was minimized. Figure 4(a) shows the net cavity transmission, along with the group delay in Fig. 4(b), neglecting additional dispersion terms due to the air gap in the etalon. The reflectivity of the mirrors was chosen to be 98%, a value that balanced the cavity finesse ( $\mathcal{F} = 155$ ) with the inherent engineering constraints that arise when designing a broadband, low dispersion mirror coating.

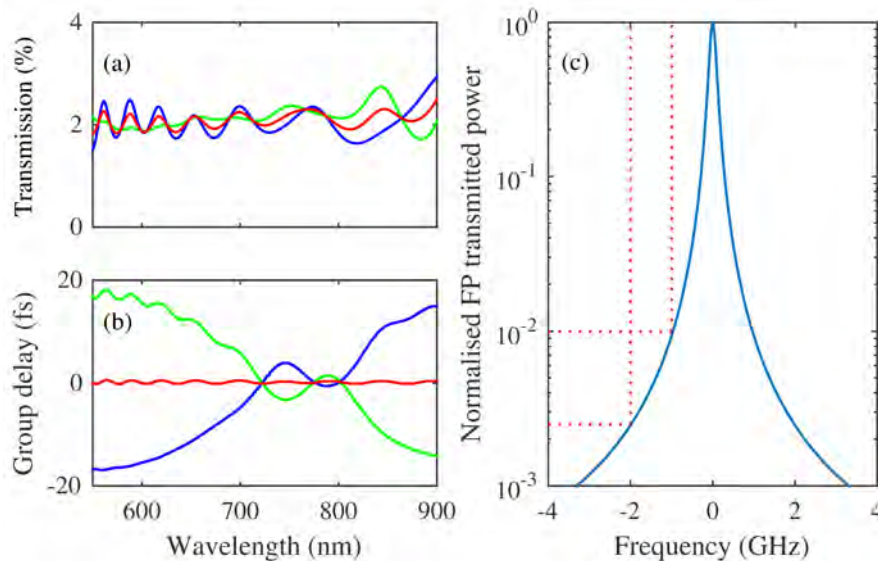


Fig. 4. Calculated transmission (a) and group delay (b) of the Fabry-Pérot filter cavity (red line) constructed from a pair of plane mirrors with complementary coatings (green and blue lines). Data courtesy of Laseroptik. (c) Modeled single-pass transmission function of the Fabry-Pérot etalon when filtering by a factor of 15. The sideband suppression is 20 dB at 1 GHz and 26 dB at 2 GHz.

The modeled single-pass transmission function of the Fabry-Pérot filter cavity is shown in Fig. 4(c). The sideband suppression at 1 GHz is 20 dB, however this does not present a significant problem for calibration of the SALT spectrograph. Unlike previously developed astrocombs, the system described here has been deployed as an instrument for improving the existing wavelength calibration, and not as a method for identifying long-term systematics and increasing the spectrograph stability. To ensure that the sideband suppression did not impact the spectrograph calibration, the Fabry-Pérot cavity was set to provide a 50 GHz comb and the filtered modes observed on the spectrograph. Even at a suppression of 10 dB, there was no measurable increase in the linewidth of the filtered comb on the spectrograph, indicating that the instrument profile had a stronger impact on the calibration than the fidelity of the comb modes.

### 3. Spectrograph calibration and results

#### 3.1 High resolution spectrograph

HRS is a fiber-fed R4 échelle spectrograph of a white pupil design with blue and red spectral channels (370-555 nm and 555-890 nm respectively) [14]. The spectrograph assembly is located within a steel tank inside a Styrofoam housing. The pressure inside the tank is kept at a constant  $5 \times 10^{-5}$  bar and the temperature controlled to within  $\pm 0.001$  K. Figure 5(a) shows the optical layout of the spectrograph. The red channel of the spectrograph is cross-dispersed onto a pair of  $2\text{kpx} \times 4\text{kpx}$  CCDs. Figure 5(b) illustrates the spectral format of the red channel, including the order numbers, blaze wavelengths ( $\lambda_B$ ), inter-order spacings ( $\Delta y$ ), and the positions of some commonly studied spectral lines. Figure 5(c) shows a 16Mpx CCD image from the red channel of HRS. The pairs of horizontal bands are the Échelle diffraction orders from these fibers, fed simultaneously with light from the comb and a payload-mounted Th-Ar lamp over a ten minute exposure. The inset panel shows the 15-GHz comb lines along with a bright Th-Ar emission line.

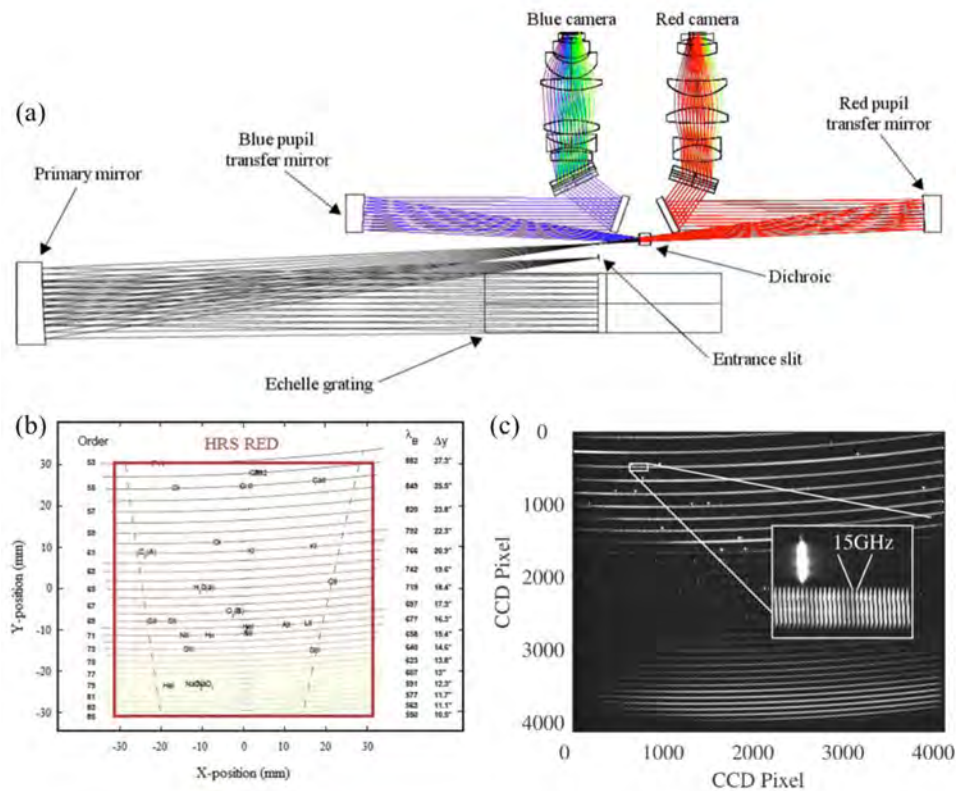


Fig. 5. (a) Optical layout of HRS. This diagram does not include the fibers that link HRS to the focal plane of the telescope or the astrocomb [14]; (b) Simulated spectral format of the red channel. Dashed lines indicate the limits of one free spectral range in each order; (c) Comparative coverage of the 15-GHz astrocomb and the payload-mounted Th-Ar lamp. The comb was coupled into the calibration channel of HRS, while the Th-Ar lamp was coupled into the object channel.

While each individual order can be extracted and fitted, complete wavelength to pixel mapping of the CCD is non-trivial due to the poor spectral coverage of the Th-Ar lamp and the nonlinear cross-dispersion within the spectrograph itself. There is scope for substantial data redundancy however, with spectral orders overlapping in the wings, as shown by the dashed lines in Fig. 5(b). The uniform frequency spacing of the astrocomb should enable

neighboring orders to be individually extracted and overlapped by aligning the teeth of the frequency comb, allowing for full spectral unwrapping of the 2D CCD into a 1D plane.

### 3.2 Improved spectral order calibration

The capability to dual-launch the Th-Ar lamp and the astrocomb provides a unique method of calibrating HRS. Here we describe how an initial calibration with the Th-Ar lamp was improved by using the co-coupled astrocomb.

The cross-dispersed spectra are recorded as a function of pixel space across the surface of the CCD. The wavelength range for each order is first determined through use of a model of the geometric dispersion of the spectrograph (see Fig. 5). Once an individual order has been selected the observed Th-Ar emission features are cross-correlated against the Th-Ar spectral atlas [19] provided by the National Optical Astronomy Observatory (NOAO) to find an initial match. Iterative matching of the HRS spectrum to the spectral atlas was then carried out until the lowest RMS error in the wavelength solution was achieved. The residuals of the comparison to the NOAO atlas, using six strong emission lines present in the HRS spectrum, are shown in Fig. 6 in red. The RMS error of the residuals was  $0.0052403(8) \text{ \AA}$ .

To improve the wavelength solution, the large number and well determined spacing of the astrocomb lines were used. For the extracted order (one with a moderate number of non-saturating Th-Ar emission lines), the exact wavelength of each of the comb lines was determined and at each of these comb lines in the HRS spectrum, a Gaussian profile was fitted to determine the position of the peak flux in the HRS spectrum. The residuals were then determined at each comb line position, and are shown in blue in Fig. 6.

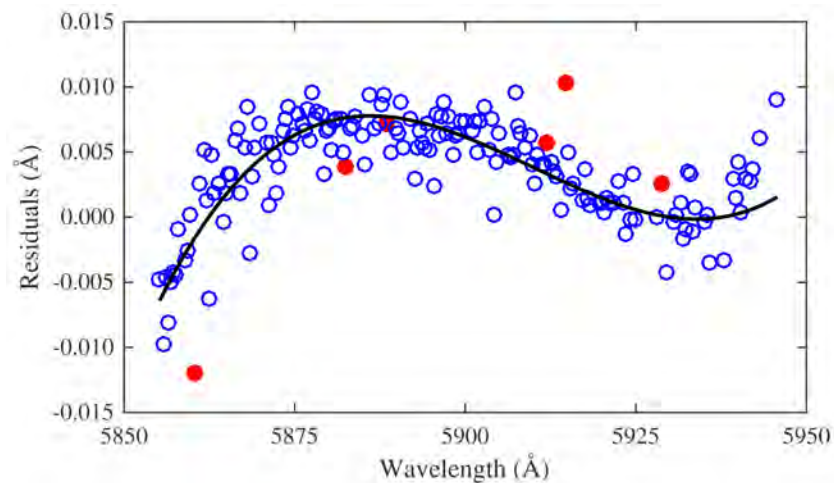


Fig. 6. Wavelength solution fitting residuals for a single order of the red channel of HRS. Residuals for a fit to six Th-Ar emission lines are shown in red, while those for the astrocomb are shown in blue. See text below for a description of the black line.

The 164 astrocomb lines used in the final fit show a clear polynomial relationship (black line) between wavelength and the residuals of the expected comb line position and the determined position of the line in the HRS spectrum when calibrated using the Th-Ar lines. This polynomial indicates the error in the Th-Ar calibration, which is limited by the availability of spectral lines. If more than six lines were available to perform a wavelength calibration, the wavelength solution might have shown the same relationship and could have been removed. Once this relationship was discovered using the large number of available comb lines and removed, a comparison to the NOAO atlas using the original six emission features resulted in an RMS of the residuals of  $0.0025867(0) \text{ \AA}$ . This factor-of-two reduction in the

error of the wavelength solution clearly demonstrates the power of having many more lines to use when performing a wavelength calibration.

A major advantage of the astrocomb over the regular Th-Ar lamp as a calibration source comes from the ability to calibrate parts of the spectrum where the Th-Ar emission features have very poor coverage, particularly in the near-infrared. In some of the orders of HRS there are no useable Th-Ar emission lines at all, with the emission features that are present being too faint (buried in the noise) or too bright (saturated) for calibration purposes. For these orders the astrocomb provides a method of wavelength calibration not available by the usual methods.

### 3.3 Improved determination of spectrograph resolution

Upon further analysis of reference [14] we have observed a previously overlooked discrepancy in the reported resolving power of two of the operating modes of HRS. The high resolution (HR) and high stability (HS) modes share the same spectrograph components, and were designed to provide a resolving power of  $R \approx 62300$  in the red channel, with the HS mode employing a fiber double scrambler prior to the spectrograph for enhanced radial velocity measurements. In [14] the resolving power of the red channel was characterized for both modes using their respective calibration sources; the HR mode was calibrating using a CalSys Th-Ar + Ar arc lamp mounted in the payload, while the HS mode was calibrated using a separate Th-Ar lamp (which we have now co-coupled into HRS with the frequency comb, as shown in Fig. 1). The analysis showed an expected deviation of the resolving power across the image plane of the CCD due to systematic effects associated with field curvature and anamorphic magnification, however there was also a significant difference between the average measured resolving powers of the two modes, with  $R_{HR} = 73700$  and  $R_{HS} = 64600$ , which the different calibration sources do not account for and the authors of [14] do not comment upon. In our astrocomb-assisted calibration of the red channel, we have addressed this discrepancy and obtained a higher measured value for the resolving power of the HS mode, as described below.

As can be observed in Fig. 5(c) and also below in Fig. 7(a), the geometric dispersion of the spectrograph produces curved spectral orders upon the surface of the CCD, with each order incident over a number of pixels in the vertical direction. Due to the curvature of the order, the Th-Ar lines used for calibration in [14] lie at an angle, covering multiple pixels in the horizontal direction. During the calibration of the HS mode carried out in [14] the pixels in each order were summed in the vertical direction to increase the signal-to-noise, however this produced an inadvertent broadening of the Th-Ar lines due to the angular tilt of the order, subsequently decreasing the measured resolving power. In our analysis we have accounted for this tilt by straightening the order during post-processing, with an example of this process shown in Fig. 7(b) using a Th-Ar lamp.

With the comb spacing tuned to 25 GHz the comb lines were clearly resolved. A Gaussian fit (Fig. 7(c)) showed a mode linewidth of 4.28 GHz, which is the convolution of the sub-MHz comb-tooth linewidth and the spectrograph response. The excellent signal-to-noise level allows for a high confidence fit ( $R^2 \geq 0.993$ ) to individual or multiple comb teeth. This value was obtained at 850 nm, implying a resolving power of  $R_{HS} = 82450$ , an enhancement of the value of  $R_{HS} = 69540$  incorrectly reported in [14] for this wavelength, and an improvement over the corresponding value of  $R_{HR} = 72420$ . In Fig. 7(d) we show the wavelength dependent resolving power of the red channel of HRS in the high stability mode. The change in the spectral resolution in the dispersion direction agrees well with similar effects reported in [14]. A higher resolution map of the resolving power for the red channel will be carried out in future experiments.

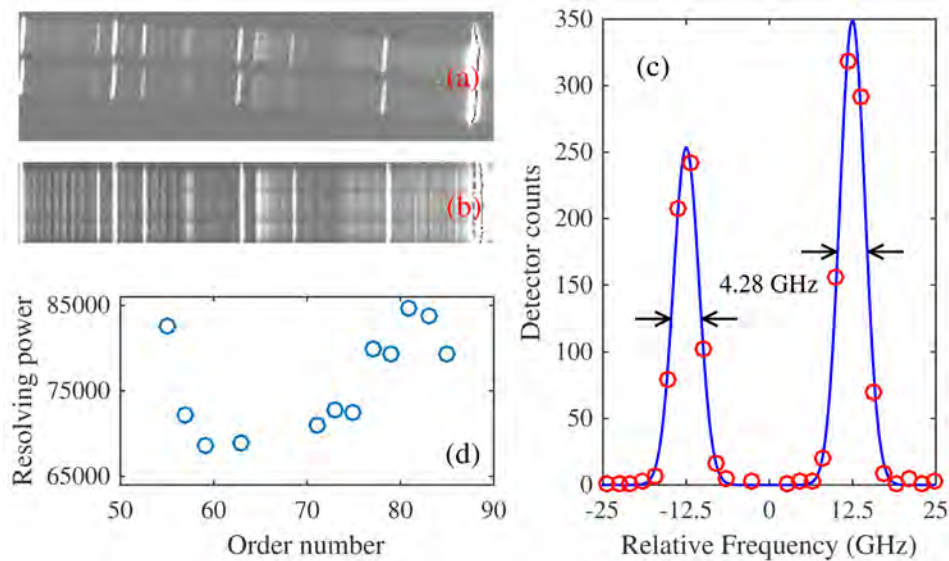


Fig. 7. Example of spectral order curvature before (a) and after (b) correction; (c) Typical Gaussian fit of the spectrograph linewidth. The 4.28-GHz full-width half maximum implies a resolving power of  $R_{HS} = 82450$  at 850nm; (d) Comb-calibrated wavelength dependent resolving power of the red channel of HRS in high stability mode.

### 3.4 Analysis of a spectrophotometric standard

We collected on-sky data with the object fiber fed by light from the spectrophotometric standard star LTT7379. In Fig. 8 we show the comb with the  $H_{\alpha}$  line from LTT7379, and the comb calibration of the star's  $H_{\alpha}$  spectrum. The comb gives an immediate measurement of the  $H_{\alpha}$  full-width half-maximum (FWHM) linewidth to be  $1.40 \text{ \AA}$  (Lorentzian fit shown in red), consistent with previous measurements of  $(1.33\text{--}1.40 \pm 0.1) \text{ \AA}$  [20]. A measurement carried out using a Th-Ar-calibrated order gives a FWHM linewidth of  $1.19 \text{ \AA}$ . The quality of the Th-Ar measurement is affected by the relatively few and faint emission lines in this order, highlighting the benefits of employing such a broadband astrocomb.

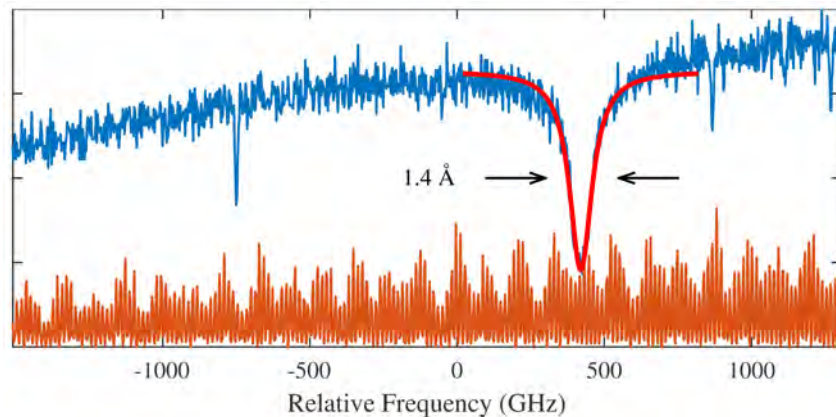


Fig. 8. Comb with mode spacing of 15 GHz (bottom) and spectrum from spectrophotometric standard star LTT7379 (top), showing the  $H_{\alpha}$  absorption feature and fit (red) inferred from the comb calibration.

#### 4. Conclusions

By measuring on-sky data using the 10-m SALT telescope we have demonstrated what is, to our knowledge, the first example of an astrocomb providing complete calibration of one channel of a high resolution astronomical spectrograph from 555 to 890 nm, fully covering the red channel of HRS where conventional Th-Ar calibration is problematic due to the sparsity and brightness variations of the available emission lines. The increased number of calibration lines per diffraction order provided by the comb reduced the wavelength-solution fitting error by a factor of two compared with a Th-Ar lamp, with a corresponding reduction in the RMS radial velocity measurement error from  $20 \text{ ms}^{-1}$  (Th-Ar lamp) to  $10 \text{ ms}^{-1}$  (comb calibration). Data reduction techniques are now being developed to fully utilize the combined atomic wavelength marker and full-channel comb scale to precisely and accurately calibrate all data from the red channel of the SALT HRS in high-stability mode, where the comb calibration revealed a previously overlooked underestimate of the resolving power of the spectrograph. It is conceivable that in the very near future, the next generation astrocombs will cover the whole wavelength range of visible spectrographs.

The development of astrocombs was originally motivated by the requirements of the most demanding astronomical observations such as radial-velocity searches for Earth-like exoplanets. While few telescopes exist with sufficiently high resolution spectrographs to address this particular science case, there are many more for which an improved spectral reference will enable new or better quality observations to be made. By covering an entire spectrograph channel the astrocomb presented in this paper addresses this technical requirement and its design has also been shown to be compatible with operation by non-specialists and in a standard telescope environment. Such architectures, possibly combined with emerging high-repetition frequency solid-state lasers [21,22] that require minimal mode filtering, will allow astrocombs to be installed at small and medium scale facilities which could immediately benefit from improved calibration.

#### Funding

UK Science and Technologies Facilities Council (STFC) (ST/N002725/1, ST/N000625/1, ST/N006925/1).